APPROACH TO A DESCRIPTIVE MODEL OF CHARGE REDUCTION IN VERMICULITE BY HYDROTHERMAL TREATMENT

ANA M. CAMPOS[†], SONIA MORENO, AND RAFAEL MOLINA*

Estado Sólido y Catálisis Ambiental (ESCA), Departamento de Química, Facultad de Ciencias, Universidad Nacional de Colombia, AK 30 No. 45-03, Bogotá, Colombia

Abstract—Vermiculites have the potential to serve as effective catalysts if pillared with Al, but their high charge presents an obstacle to the pillaring process. The purpose of this study was to submit natural vermiculite to thermal treatments in the presence of water vapor in order to effect a reduction in the global negative charge and thereby to enhance its susceptibility to pillaring. The process of charge reduction in vermiculite under the conditions selected involved the extraction of 25% of ^{IV}Al accompanied by the extraction of structural Mg and charge-compensating cations (Ca^{2+}, Na^+, and K^+). The results indicate a reduction of 35% in the global negative charge in vermiculite by the end of the treatment. Some of the ^{VI}Al content was not removed during acid washing, and probably remained in the solid in structural positions in the octahedral sheet.

Key Words—Hydrothermal Treatment, Layer Charge, Pillared Clay, Vermiculite, Water Vapor.

INTRODUCTION

The large negative charge generated by the elevated isomorphic substitutions of silica by Al in the tetrahedral sheet in vermiculite is an obstacle to the conventional cationic exchange process, which is the first step to obtaining a pillared clay. The limited number of attempts to pillar vermiculite is a result of this problem (d'Espinose de la Calleire and Fripiat, 1991; Michot *et al.*, 1994; Campos *et al.*, 2005). Recent development of efficient methods to achieve charge reduction have allowed for the pillaring of vermiculite, *e.g.* acid treatment (del Rey-Perez-Caballero and Poncelet 2000; Chmielarz *et al.*, 2008), liquid-phase ultrasonic treatment in the presence of H_2O_2 (Jiménez de Haro *et al.*, 2005; Wiewióra *et al.*, 2003), and most recently the application of a hydrothermal treatment (HTT) (Cristiano *et al.*, 2005).

The immediate consequence of submitting vermiculites to a HTT process is an efficient reduction in the negative charge, which makes possible a cationic exchange process and subsequently the pillaring process, as observed by Cristiano *et al.* (2005) and by Campos *et al.* (2008). In order to study the HTT process, systematic study of the main parameters involved is essential to determine their effect on the structural and catalytic properties of the pillared mineral.

The aim of the study was, therefore, to study the application of HTT to natural vermiculite, emphasizing the effects of both the relative humidity and the temperature. The particle size of the untreated material and water-vapor-flow effects on the HTT process were reported by Campos *et al.* (2008).

EXPERIMENTAL

The initial material, labeled V, is a natural Colombian vermiculite (from the Santa Marta region) which has been fully characterized (Campos *et al.*, 2005; Cristiano *et al.*, 2005; Campos, 2007). The structural formula for the mineral is $[(Si_{3.04}Al_{0.92}Ti_{0.04})(Al_{0.11}Fe^{3+}_{0.35}Fe^{2+}_{0.07}Mg_{2.41}Mn_{0.003})O_{10}(OH)_2]Ca_{0.21}K_{0.05}Na_{0.10}$ (Campos, 2007).

The V was submitted to HTT under different conditions selected from a previous study (Campos *et al.*, 2008) in order to assess the effect of both the relative humidity and temperature on the negative charge density and the capacity to generate pillaring structures. To assess the pillaring process, the solids were pillared with Al. Evaluation of the thermal effects was achieved mainly through use of X-ray diffraction (XRD), and of the catalytic performance by heptane hydro-conversion.

Some solids were selected for detailed characterization by means of cation exchange capacity (CEC), X-ray fluorescence (XRF), N_2 adsorption/desorption isotherms, Al nuclear magnetic resonance ^{27}Al-NMR, X-ray photoelectron spectroscopy (XPS), and diffuse reflectance infrared spectroscopy (DRIFT).

Hydrothermal treatment

In the HTT process the material was loaded into a fixed-bed reactor (15 g of clay) and submitted to the desired temperature at a heating speed of 5ºC min^{-1}. Once the temperature had been reached, a N_2 flow with water vapor, generated through a saturator filled with distilled water at a temperature required to obtain the desired relative humidity in nitrogen, was circulated for

* E-mail address of corresponding author:
ramolinag@unal.edu.co
[†] Present address: Departamento de Ciencias Básicas, Universidad Jorge Tadeo Lozano, Bogotá, Colombia

6 h (Cristiano *et al.* 2005). In all cases, the removal of species that could be extracted from the clay layers and retained on the surface of the solid during the HTT process was carried out with 0.25 M nitric acid (10 mL g^{-1} clay) under constant stirring for 1 h at 80ºC. The solids were finally washed with distilled water and dried at 60ºC.

Relative humidity and temperature

In order to assess the effect of the temperature and relative humidity in N$_2$, a statistical model was proposed in which the parameters to cover extreme conditions for the evaluation of the HTT process could be combined. Temperatures of 200, 300, and 400ºC and relative humidity in N$_2$ of 25, 50, and 75% were used. Use of these six parameters allowed for nine possible experimental combinations.

The experiments were carried using the <150 μm fraction with a constant-weight hourly space velocity (WHSV) of 60 g water g^{-1} catalyst h^{-1}, with values selected from the results obtained previously (Campos *et al.*, 2008).

Naming of the solids corresponded to the temperature-name of the clay-water-relative humidity; *i.e.* solid 400V50 corresponds to the solid obtained from vermiculite submitted to the HTT process at 400ºC and with relative humidity of 50% in N$_2$. The solids obtained after acid washing are distinguished by the prefix H, so H400V75 corresponds to the solid originating from the HTT process in 400V75 conditions, and then washed with acid.

Selection of solids

In order to establish an approximation to the descriptive model for the reduction of the interlayer charge in the vermiculite through the HTT treatment, a complementary analysis in four catalysts (200V25, 300V50, 400V75, and H400V75) was carried out, as they were considered to be representative of the behavior of the experimental conditions selected.

Pillaring with Al

The Al polymer solutions were prepared to obtain 12 mmol of Al g^{-1} clay (del Rey-Perez-Caballero and Poncelet, 2000) by dropwise addition of a 0.4 M solution of NaOH to an AlCl$_3$ 0.4 M solution while the temperature of the solution was increased to 80ºC, and by using a molar OH:Al ratio of 2. After aging for 36 h at room temperature, the pillaring solution was slowly added to a clay suspension (2 wt.%) under vigorous stirring. The temperature during the exchange was 80ºC and was maintained for 4 h at the end of the addition. The final suspension (clay and pillaring solution) was aged for 12 h. Finally, excess salt was reduced through washing with distilled water. The clays were dried at 60ºC and calcined at 400ºC (5ºC min^{-1}), maintaining this temperature for 2 h. The solids obtained after

pillaring are referred to as Al-PILV, and the particular nomenclature was a function of the different treatments to which they were submitted.

Characterization

The CEC was determined on clays previously exchanged with ammonia acetate solution under reflux conditions, by means of the micro-Kjeldahl method (Chapman, 1965). The chemical analysis was carried out by means of X-ray fluorescence (XRF) using an FRX Philips Magix Pro PW 2440.

X-ray diffraction was carried out on powders after the HTT process using a Philips PW 1820 diffractometer (CuKα radiation, λ = 1.54056 Å, 40 mA, 40 kV) in º2θ geometry and Bragg-Brentano configuration using a step size of 0.05º2θ and a step time of 2 s.

The specific surface area was determined from the N$_2$-adsorption isotherm at the temperature of liquid nitrogen by means of a Micromeritics Tristar 3000 instrument. Before the measurements, the samples were outgassed by heating to 400ºC under a residual vacuum of 0.01 Pa. The data were recorded at P/P_0 between 0.0005 and 0.99.

The ^{27}Al nuclear magnetic resonance spectra were obtained using a Bruker Advance spectrometer 400. The solids were placed in 2.5 mm rotors, while 1200 sweeps were accumulated in a time of 100 ms of recycling. The rotor speed was 5000 Hz.

X-ray photoelectron spectroscopy was performed by means of a Kratos Axis Ultra spectrometer (Kratos Analytical, Manchester, UK), with a monochromatic Al source. The analysis pressure in the chamber was 10^{-6} Pa. The angle between the sample surface and the direction of the photoelectrons was 0º. The energy range scanned was fixed at 160 eV for a wide sweep and at 40 eV for a narrow sweep. Under these conditions, the FHWM (full width at half maximum) for the standard Ag 3$d_{5/2}$ signal was 1.0 eV. The following photoelectron energies were observed: C1s, O1s, Mg2s, Si2p, Al2p, Fe2p, Na1s, K2p, and C1s. The spectra were calibrated using the C1s signal at 284.8 eV as an internal standard. Elemental molar fractions (%) were calculated on the basis of acquisition parameters after a linear background subtraction of experimental sensitivity factors (Wagner, 1990) and transmission function provided by the manufacturer.

The DRIFT spectra were recorded in the middle-IR region (4000−400 cm^{-1}) using a Bruker Equinox55 spectrometer with a DTGS KBr detector (resolution 4 cm^{-1}, 32 scans) at ambient conditions on previously degassed clay powders purged with N$_2$ at 10 mL min^{-1} for 1 h at 400ºC.

Catalytic evaluation

The catalytic behavior of the different solids was assessed by means of heptane hydro-conversion. Taking into account the bifunctional nature of the reaction and the 'ideal' metal/acid balance reported (Moreno *et al.*,

1996, 1997), catalysts were impregnated with a solution of tetraamine platinum(II) chloride, using the volume of the solution required to obtain 1 wt.%. The clays were then compressed to pellets. Particles with average diameters between 125 μm and 250 μm were selected. Activation of the solid and the catalytic test were performed in a fixed-bed reactor at atmospheric pressure following conditions reported previously (Cristiano *et al.*, 2005; Hernández *et al.*, 2008a, 2008b; Campos *et al.*, 2008). With this purpose, the solid (0.2 g) was raised to a temperature of 400ºC at a speed of 10ºC min^{-1} with a flow of dry air for 2 h; then the circuit was purged with N_2 for 15 min. Later, reduction of metal was performed by purging with H_2 (pure hydrogen) at the same temperature for 2 h. The reactor was then cooled and stabilized at 150ºC. The flow of heptane was generated by the passing of H_2 through a saturator containing the reagent at 27ºC. The total flow of hydrogen/heptane was 10 mL min^{-1} and the WHSV of 1.2 g of heptane g^{-1} catalyst h^{-1}. The reaction was performed over the temperature range 150ºC to 400ºC at a heating rate of 0.9ºC min^{-1}. Analysis of the reaction products was performed by gas chromatography with GC-17 equipment, fitted with a HP-1 (5 m × 0.53 mm × 0.52 μm) column and an FID detector.

RESULTS AND DISCUSSION

A systematic study of the global effects of charge reduction in vermiculites by the application of the HTT process was performed, starting from the experimental conditions selected in previous studies (Cristiano *et al.* 2005; Campos *et al.* 2008), which were temperatures between 200 and 400ºC and a relative humidity of 50% in N_2.

The effect of relative humidity and temperature

The effect of the HTT process as a function of the temperature on untreated vermiculite, V, keeping the relative humidity constant (Figure 1) indicated that the solid subjected to HTT at 50% relative humidity exhibited typical behavior. In the first step of the charge-reduction treatment, the HTT clearly revealed no significant changes in the starting vermiculite, as the basal reflection characterizing the clay mineral was preserved (Campos *et al.*, 2008). The most notable effect observed was the reduction in intensity and broadening of the reflections, particularly those of first order, and a slight shift of the d_{001} peak to 1.41 nm in the 400V50 solid with respect to the natural vermiculite, located at 1.43 nm (Campos *et al.*, 2007). The shift may be related to a reduction in negative charge, which is accompanied by a reduction in the interlayer spacing (Komadel *et al.*, 2005) and disturbs the layer stacking in vermiculite (Tunega and Lischka, 2003).

Acid washing can cause particle-size reduction, dissolution of layers, large surface areas (Maqueda *et al.* 2008), or selective Al extraction (del Rey-Perez-Caballero and Poncelet 2000), depending on the conditions (*e.g.* acid concentration, temperature, and time of washing) during the treatment. The behavior of all solids (clays 200V50 to H200V50) before and after acid washing (Figure 2) confirmed these expectations. The apparent slight broadening of the d_{001} peak could also imply a decrease in negative charge. After acid washing, an increase in the HTT temperature led to more broadening of the d_{001} peak and a more noticeable reduction in the remaining reflections (Figure 3). For an increase in the relative humidity when the HTT temperature was constant (400ºC), the effect was not
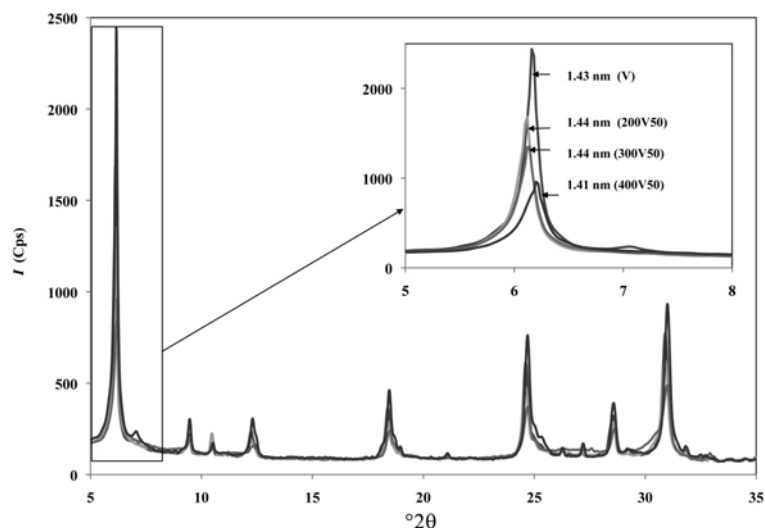

Figure 1. XRD patterns of natural vermiculite after the HTT process at 50% relative humidity and different temperatures.
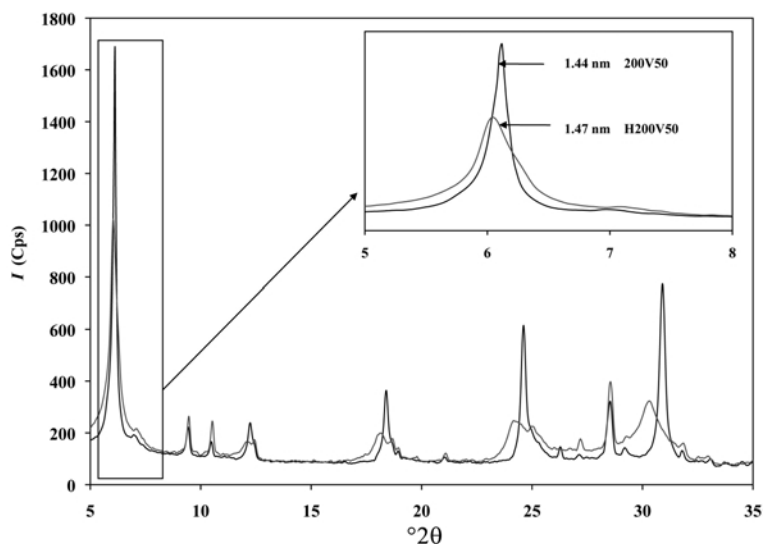
Figure 2. XRD patterns of vermiculites 200V50 and H200V5.

substantial, as suggested by the slight reduction in the intensity of the signals and unchanging basal spacings of the materials (Figure 3).

Simultaneously, and in order to verify the negative charge reduction in vermiculite, the total CEC was determined and a chemical analysis (XRF) was performed after each of the steps for the charge reduction of the initial clay. Results (Table 1) revealed a modification in the CEC, indicating a reduction in negative charge with respect to the natural clay mineral. At the end of the HTT process and after acid washing, charge reduction of between 30 and 45% with respect to the untreated V was observed.

The reduction in CEC was consistent with a permanent reduction in the global negative charge (Komadel *et al.*, 2005). The effect of temperature was revealed by a more significant reduction in the CEC at the largest value (400ºC). With respect to the relative humidity, the differences among solids were less significant with the largest reduction in CEC being achieved in solid H400V75.

XRF analysis performed on the V sample after the HTT and acid washing (Table 2) found a reduction in the Al content (an increase in the Si:Al ratio) with respect to the natural V, which proves that the extraction of this element during the HTT process was the most relevant factor in the reduction of charge. The reduction in the Al and Mg contents (Table 2) indicates that the process probably involved the breaking of O−Mg−OH bonds in the octahedral sheet, and of Si−O−Al bonds in the tetrahedral sheets, and some of the structural elements (Al, Mg) can be completely extracted in the acid solution, as has been proposed for acid-treated vermiculites (del Rey-Perez-Caballero and Poncelet, 2000). The SiO_2 and Fe_2O_3 contents increased after the HTT process and acid washing with respect to the untreated samples, possibly because they are less soluble.

On the other hand, the increase in temperature and relative humidity led to the smallest reduction in the Al content and, as a result, to a larger Si:Al ratio, which accounts for the change in the solid H400V75 being the most significant with respect to the initial clay mineral (V).

The effect of relative humidity and temperature in the HTT process on the pillaring (Al-PILV)

The XRD patterns for the pillared samples Al-PILV, obtained from vermiculites submitted to HTT at different temperatures and with the same relative humidity (75%) (Figure 4) revealed that an increase in temperature increases the intensity of the reflection corresponding to the basal spacing of vermiculites which were successfully pillared with Al, indicating the more crystalline nature and/or distribution of the pillars in the interlayer spacing (Moreno *et al.*, 1996).

Table 1. CEC of natural vermiculite, vermiculites after the HTT process, and acid washing

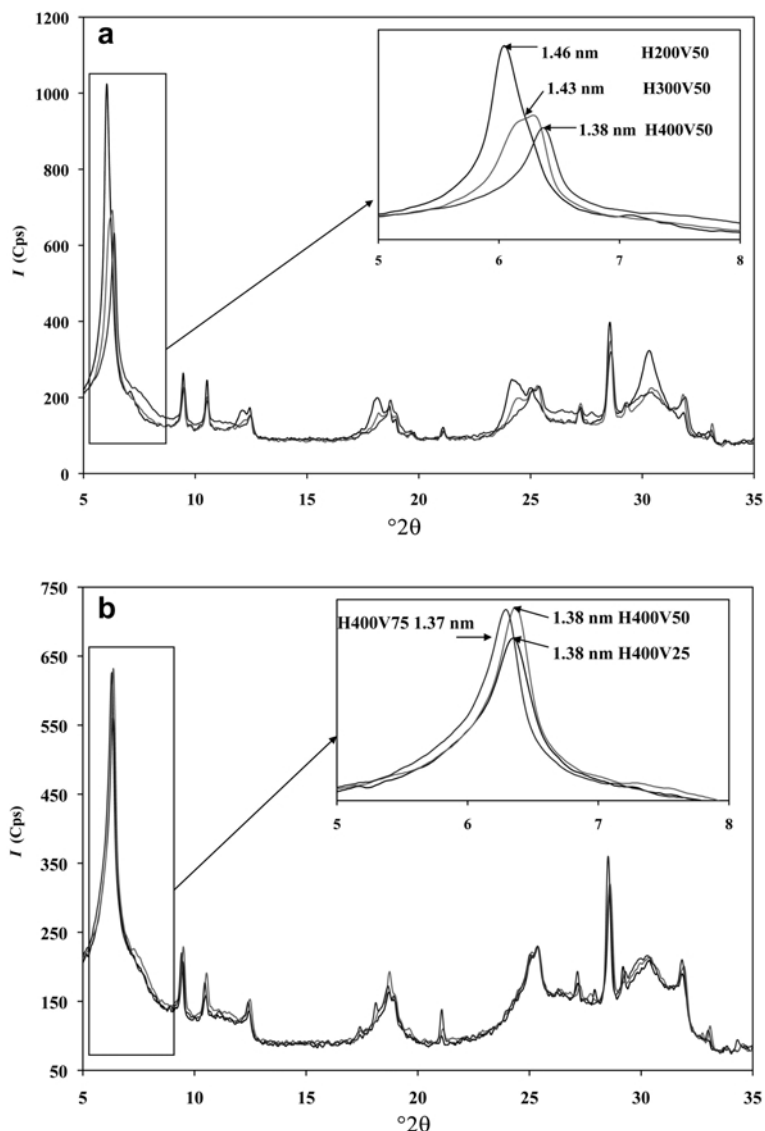| Clay	CEC (meq 100 g^{-1})
V	110
H200V25	81.2
H200V50	80.1
H200V75	79.2
H300V25	81.1
H300V50	79.4
H300V75	82.9
H400V25	76.2
H400V50	65.4
H400V75	61.7

Figure 3. XRD patterns of vermiculites after HTT and acid washing, selected at different temperatures and 50% relative humidity (a); and at a temperature of 400ºC with different relative humidities (b).

Table 2. Chemical analysis of the vermiculites by X-ray fluorescence (wt.%) after the HTT process and acid washing.

| Clay	Al_2O_3	SiO_2	CaO	Fe_2O_3	K_2O	MgO	Na_2O	P_2O_5	TiO_2	Si/Al
V	13.1	45.4	2.9	8.1	0.6	24.1	0.2	0.3	0.7	2.94
H200V25	11.7	46.3	2.3	8.8	0.4	22.9	0.2	0.1	0.7	3.36
H200V50	11.2	47.1	2.6	8.7	0.4	22.7	0.2	0.1	0.7	3.56
H200V75	11.2	46.9	2.7	8.7	0.4	22.8	0.2	0.2	0.7	3.54
H300V25	11.1	47.9	3.0	8.9	0.4	22.7	0.3	0.2	0.8	3.65
H300V50	10.9	46.3	2.8	8.6	0.4	22.2	0.2	0.2	0.7	3.60
H300V75	10.8	46.9	2.9	8.7	0.4	22.3	0.3	0.2	0.8	3.69
H400V25	11.1	47.0	2.7	8.7	0.4	22.5	0.2	0.2	0.7	3.59
H400V50	10.8	47.5	2.9	8.7	0.4	22.5	0.3	0.2	0.8	3.73
H400V75	10.6	47.8	2.2	8.4	0.4	20.8	0.2	0.1	0.7	3.80
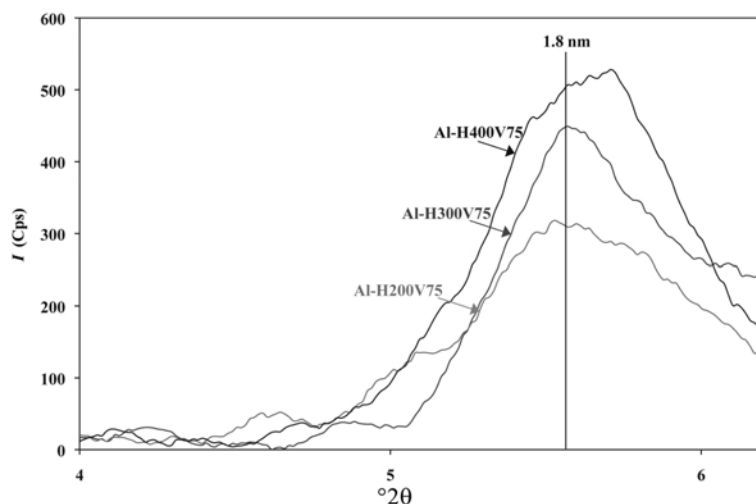
Figure 4. XRD patterns of Al-pillared vermiculites, starting from vermiculites subjected to the HTT process at 75% relative humidity and different temperatures after acid washing.

An increase in the relative humidity (25%, 50%, and 75%) in the HTT process for pillared samples Al-PILV, evaluated at 400°C, clearly favors the pillaring process, as indicated by a greater intensity in the XRD pattern of the d_{001} peak obtained at 75% (Figure 5).

With reference to the catalytic behavior of heptane conversion (Figure 6), the general tendency suggested that an increase in the temperature of the HTT improved the charge reduction and, therefore, led to a better pillar distribution between the layers. Better catalytic performance in a pillared clay is the result of such a characteristic (Moreno *et al.*, 1996). The parameters of catalytic activity in heptane conversion on Al-vermiculites obtained after the HTT process at different conditions (Table 3) clearly revealed the beneficial effects of increasing the relative humidity and tempera-ture, initially through a reduction in the T_{10ISO} and T_{max} in the 300 and 400°C series. The parameters indicated greater accessibility to active acid sites (Moreno *et al.*, 1997), favoring the conversion at lower temperatures. Such behavior may also be related to different degrees of dealumination achieved during the HTT, which may generate a greater quantity of strong acid sites of the Brönsted type remaining in the Si−O−Al units associated with the tetrahedral sheets (Tunega and Lischka, 2003).

Finally, the best structural and catalytic properties were observed in the pillared sample Al-PILV from the H400V75 conditions. The solid was characterized by a greater reduction in CEC and a greater Si:Al ratio, suggesting a more efficient charge reduction and, consequently, a more successful pillaring process.
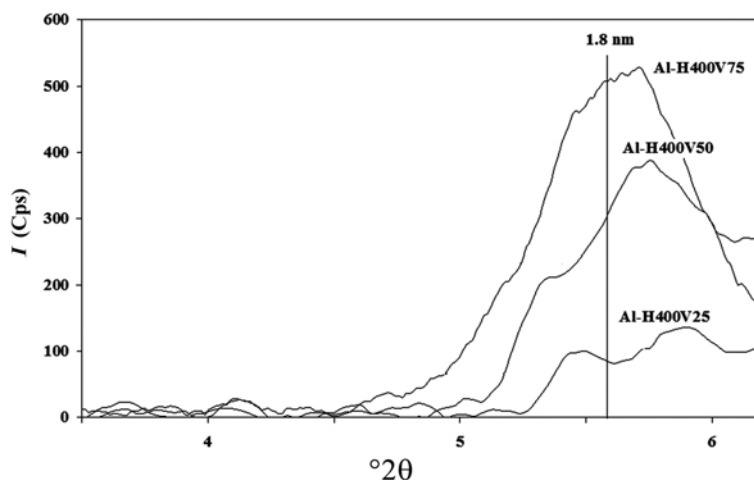

Figure 5. XRD patterns of Al-pillared vermiculites after the HTT process at 25%, 50%, and 75% relative humidity, a temperature of 400°C, and after acid washing.
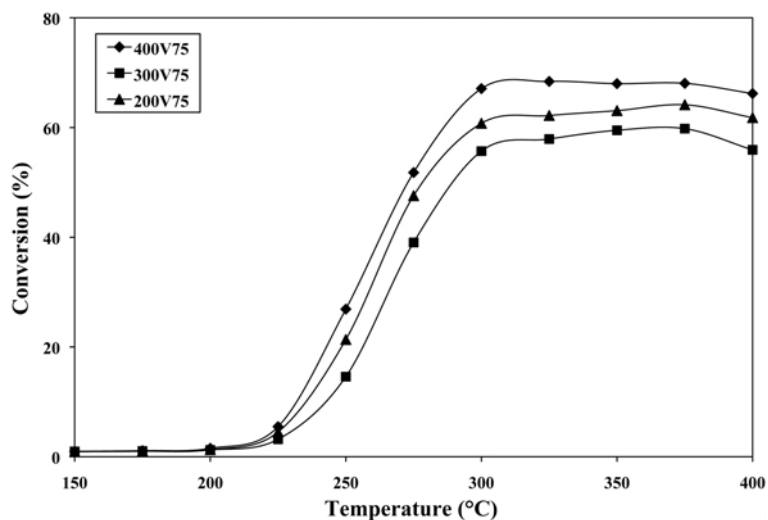
Figure 6. Heptane conversion on Pt/Al-vermiculites after the HTT process at different temperatures and a constant relative humidity (75%).

Complementary structural characterizations

Once the optimal parameters for the HTT application had been selected (400V75), complementary analyses were carried out on the sequence of conditions V, 400V75, and H400V75. In addition, the solids 200V25, 300V50, and 400V75 were selected as representative of the behavior of solids submitted to the HTT process.

^{27}Al Nuclear magnetic resonance

The clays selected for complementary analysis were examined using ^{27}Al MAS-NMR spectroscopy in order to examine the coordination of Al during the HTT process. The NMR spectra of the initial vermiculite, V, (Figure 7) show two signals at 0 and 60 ppm, due to ^{VI}Al and ^{IV}Al, respectively (Klinowski, 1999).

After hydrothermal treatment, an increase in the 0 ppm signal and a reduction of the 60 ppm signal were observed in sample 400V75, evidence of the increase in

^{VI}Al and confirming the extraction of Al from the tetrahedral sheet. The same effect was not noted for solids 200V25 or 300V50. The mathematical compositions of the spectra (Table 4) confirmed the extraction of Al, with an increase in the $^{VI}Al:^{IV}Al$ ratio in solid 400V75.

In sample H400V75, the increase in the ^{VI}Al signal was more significant with respect to the initial clay, V, as confirmed by the area of this species (Table 4). On the other hand, the ^{VI}Al signal was shifted slightly (by 4 ppm), suggesting the presence of different extra-framework species (del Rey-Perez-Caballero and Poncelet, 2000) or a different chemical environment for the Al located in the octahedral sheet (Figure 7) (Komadel et al., 2005).

The increase in the ^{VI}Al species after acid washing was unexpected, since its solubility in this medium is widely acknowledged (Giudici et al., 2000). Although ^{VI}Al

Table 3. Parameters of catalytic evaluation of heptane hydro-isomerization of Al-vermiculites after the HTT process.

HTT conditions	T_{10ISO}[a] (°C)	T_{max}[b] (°C)	Conv[c] (%)	Y_{CR}[c] (%)	Y_{ISO}[c] (%)	Sel_{ISO}[c] (%)
200V25	250	325	48.5	7.1	41.3	85.2
200V50	250	325	57.4	15.2	41,2	71.8
200V75	250	325	60.8	6.5	54.3	89.3
300V25	250	325	53.6	10.3	43.2	80.6
300V50	245	300	54.2	6.21	47.9	88.4
300V75	245	300	55.7	5.01	50.7	91.0
400V25	245	300	52.3	6.4	46.5	88.9
400V50	235	300	63.8	6.4	49.0	76.8
400V75	225	300	71.9	14.7	57.3	79.7

[a] The temperature at which the catalyst reaches 10% isomerization.
[b] The maximum isomerization temperature.
[c] Total conversion Conv, cracking yield Y_{CR}, isomer yield, Y_{ISO}, and the selectivity to heptane isomers Sel_{ISO} at T_{max}.
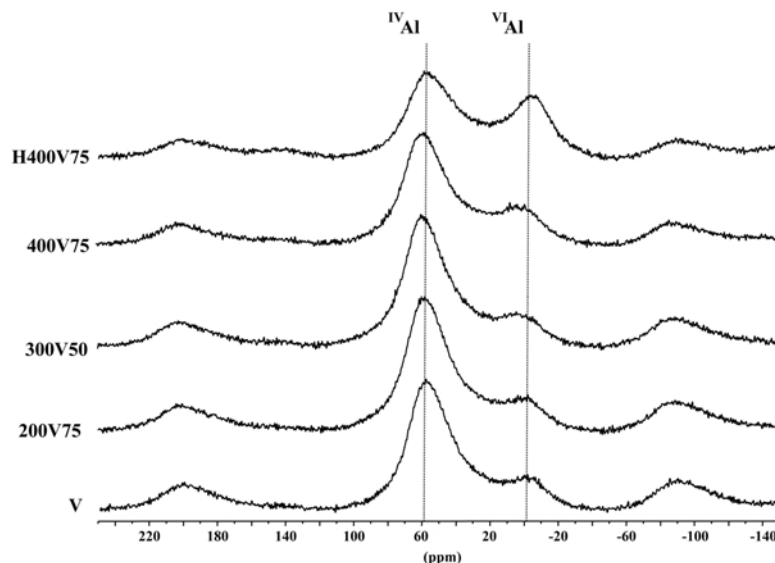
Figure 7. ^{27}Al-NMR spectra of natural vermiculite (V), vermiculites after the HTT process under the conditions 400V75, 300V50, and 200V25, and vermiculite with acid washing after HTT under conditions 400V75 (H400V75).

species can remain on the solid surfaces after acid washing (del Rey-Perez-Caballero and Poncelet, 2000; Triantafillidis *et al.*, 2000), Al extracted from the tetrahedral sheet could have migrated during the HTT process (del Rey-Perez-Caballero and Poncelet, 2000) towards the closest vacant sites in the octahedral sheet, thanks to their small ionic radius (Tunega and Lischka, 2003; Chorom and Rengasamy, 1996). The present technique does not allow the framework or extra-framework quality of the ^{VI}Al species of the clay to be defined.

The results strongly indicate that charge reduction in vermiculite is caused by the extraction of as much as 25.4% of ^{IV}Al; but, at the end of the treatment, some of the Al remains in the clay structure in spite of the acid washing.

X-ray photoelectron spectroscopy

X-ray photoelectron spectroscopy results of vermiculites after the HTT process (Table 5) revealed dealumination through an increase in the Al content in the

sample surface layers with respect to the starting clay, V. Enrichment of Fe in the surface layers indicated that it also may have been extracted during the HTT process but remained on the sample surface.

With respect to Al 2p binding energy, an average increase of ~0.4 eV was observed with respect to the untreated clay mineral, V (Table 5). If most of the Al corresponds to ^{IV}Al according to NMR analysis, the behavior suggests that the increase in the Si content gives rise to an increase in the ionic nature of the Al—O bonds remaining in the tetrahedral sheet (Barr *et al.*, 1997) and, as a consequence, the XPS signal was shifted.

For material after the HTT process and acid washing (H400V75), an increase was observed in the Si:Al, Si:Mg, and Si:Fe ratios (Table 5) compared with the unwashed material (400V75), indicating the extraction of these ions from their structural positions in the clay after the acid washing.

The effect of dealumination on the vermiculite structure was also revealed in the Si 2p signal. The values of the binding energies for Si 2p and the O 1s (Figure 8) for the solids V, 400V75, and H400V75 revealed a good correlation, indicating a common origin for the shift in these two photoelectron energies. The behavior was also evident in "laminar silicates" (Gonzalez *et al.*, 1988), and suggests that the SiO_4^{4-} units were sensitive to changes in the electron density expected during the HTT process in vermiculite.

The shift in the Mg 2s signal (0.6 eV) in sample H400V75 compared with V suggests that a modification in the organization of the octahedral sheet was clearly generated by the HTT process, which may modify the chemical environment of the principal cation in the sheet.

Table 4. Areas of ^{IV}Al and ^{VI}Al peaks in the ^{27}Al-NMR spectrum for natural vermiculite and for vermiculites after the HTT process.

Clay	^{VI}Al	^{IV}Al	Ratio ^{IV}Al:^{VI}Al
V	8.8	91.2	10.4
200V25	8.9	91.1	10.2
300V50	8.7	91.3	10.5
400V75	12.6	87.4	6.9
H400V75	24.6	75.4	3.1

Table 5. XPS data and relative atomic ratios for natural vermiculite and samples after the HTT process.

Signal		Clay				
		V	200V25	300V50	400V75	H400V75
Na1s	%	0.2	0.1	0.1	0.1	0.1
	BE (eV)	1072.6	1073.0	1072.9	1072.5	1072.1
Fe2$p_{3/2}$	%	2.8	3.5	3.4	3.8	3.5
	BE (eV)	712.2	712.3	712.5	712.6	712.5
O1s	%	54.8	56.8	57.2	57.8	57.5
	BE (eV)	531.6	531.9	531.9	532.0	532.3
K2p	%	0.1	0.2	0.2	0.2	0.2
	BE (eV)	293.1	293.4	294.0	293.2	293.6
Si2p	%	16.6	16.6	17.8	17.4	18.8
	BE (eV)	102.6	102.8	103.1	102.8	103.1
Al2p	%	4.1	5.0	4.9	5.0	4.8
	BE (eV)	74.1	74.5	74.7	74.2	74.5
Mg2s	%	7.4	7.7	7.5	7.3	6.8
	BE (eV)	88.7	88.8	89.2	89.0	89.3
Ratios	Si:Al	4.0	3.3	3.6	3.5	3.9
	Si:Mg	2.2	2.2	2.4	2.4	2.8
	Si:Fe	5.9	4.7	5.2	4.6	5.4

BE: binding energy

Diffuse reflectance infrared Fourier transform spectroscopy (DRIFT)

Study of DRIFT spectra during the HTT process helps determine changes in vermiculite by observing the featured vibrations of minerals in the IR region, especially in the intense Si-O vibrational bands ($1200-1100$ cm^{-1}) (Marques $et\ al.$ 2005).

The DRIFT spectra of the V, 400V75, and H400V75 (Figure 9) showed a decrease in the intensity of the 914 cm^{-1} peak. A shift in the Si$-$O vibration from 1200 cm^{-1} in V to 1236 cm^{-1} in the solid H400V75 was also observed. The behavior of the Si$-$O vibration is directly related to the process of dealumination in the clay tetrahedral sheet, as reported by other authors (Kitajima $et\ al.$, 1991; Madejová $et\ al.$, 2000) who

concluded that a reduction in the laminar charge in smectites occurred because of the fixing of cations such as Li^{+}. The general conclusion has been that the Si$-$O vibrations reflect structural aspects of the SiO$_4^{4-}$ units, which are influenced by the magnitude of the laminar charge and its location (Madejová $et\ al.$, 2000). In the case of vermiculite, the shifting of this vibration provides additional evidence for the extraction of ^{IV}Al, modifying the environment for SiO$_4^{4-}$ units (Si:Al ratio) and, consequently, reducing the laminar charge.

The considerable reduction in the intensities of the bands located in the 914 and 630 cm^{-1} regions may be related to changes occurring in the octahedral sheet during HTT, due to the fact that this region derives from the perpendicular vibrations of the octahedral ions, $i.e.$ of the $R-$O$-$Al (R = Fe or Mg) groups (Madejová $et\ al.$, 1998).

With respect to vibrational stretching of hydroxyl groups, the appearance of a peak at 3720 cm^{-1} is mainly observed in the solid H400V75, which has been assigned to new Si$-$OH groups (Moreno $et\ al.$, 1997).

Nitrogen absorption/desorption

Nitrogen adsorption/desorption isotherms (Figure 10) clearly reveal significant changes in the textural properties of natural clay when submitted to the HTT process. Clay V shows a type II isotherm according to the IUPAC classification (Sing $et\ al.$, 1985), with a type 4 hysteresis which is often given by aggregates of platy particles or adsorbents containing slit-shaped pores. The same behavior was observed in the clay after the HTT process (400V75).
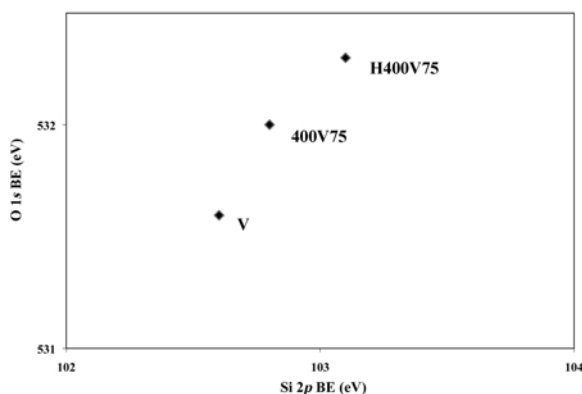

Figure 8. Relation between the binding energy (BE) of Si2p and O1s in the samples V, 400V75, and 550 H400V75.
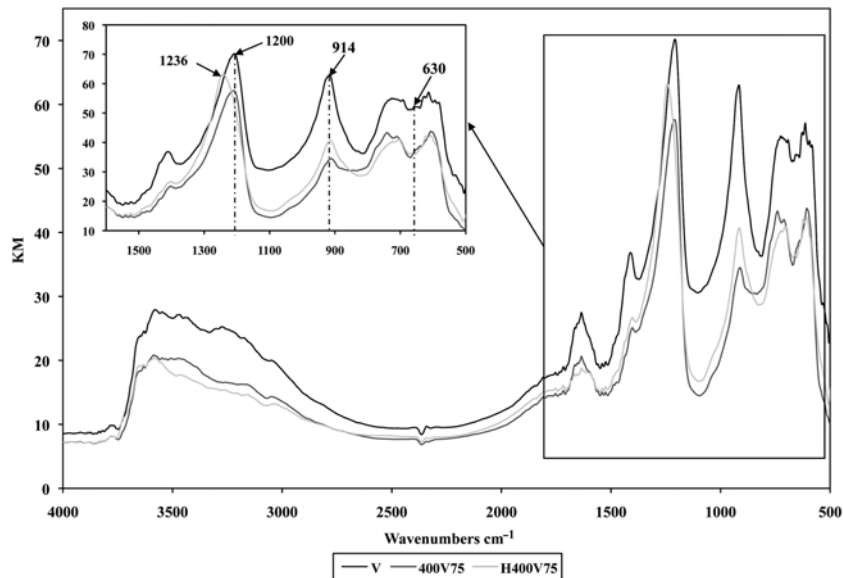
Figure 9. DRIFT spectra of samples of initial vermiculite (V), 400V75, and H400V75.

After acid washing, a larger capacity for adsorption as a consequence of the generation of microporosity was revealed in the adsorption isotherm for the solid H400V75 (Table 6), which corresponds to a type I isotherm and a type 4 hysteresis (Sing *et al.*, 1985).

The increase in the adsorption may be related to the charge reduction which generates expansion in the interlayer space and, therefore, enhances the adsorption power of the clay. The results confirm the significant effect of the textural properties of vermiculite at the end of the HTT (Table 6).

Approach to a descriptive model of charge reduction by the HTT process in vermiculite

The results show that during treatment, the most significant effect is the extraction of Al, evident from an increase in the Si:Al ratio and from the shift in the Si–O vibration from 1200 cm^{-1} in the untreated clay mineral to 1236 cm^{-1} in the H400V75 solid. A reduction in the negative charge of vermiculite was confirmed by the ~35% reduction in its CEC.

Reduction of Al and Mg according to elemental analysis suggests that the process probably started with
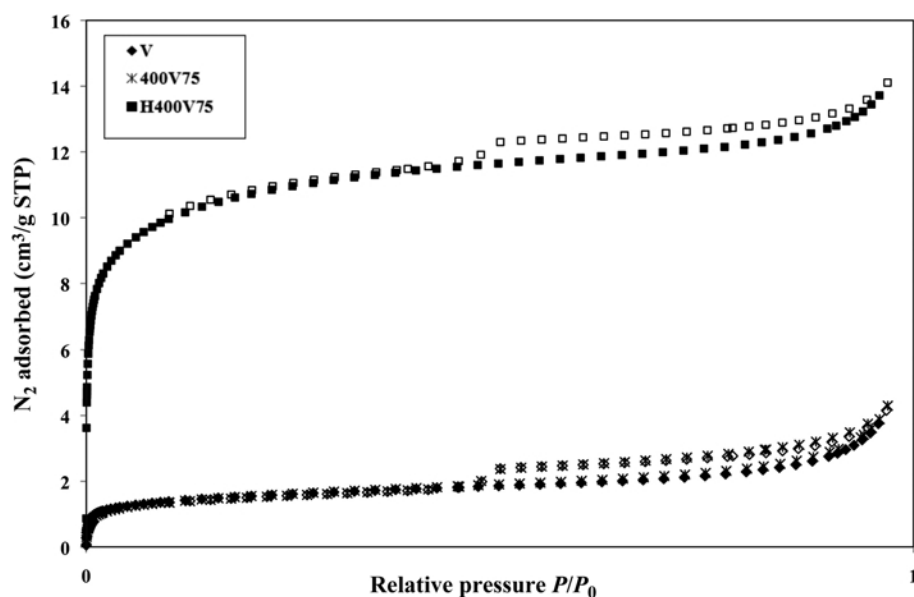

Figure 10. Adsorption isotherms of nitrogen on the vermiculites V, 400V75, and H400V75.

Table 6. Textural data in natural vermiculite and samples after the HTT process.

Clay	S_{BET} $(m^2\ g^{-1})$	V micro $(cm^3\ g^{-1})$	Area micro $(m^2\ g^{-1})$
V	7.4	0.001	4.3
400V75	7.5	0.002	4.1
H400V75	44.6	0.016	29.4

breaking of the O−Mg−O bonds in the octahedral sheet and in the Si−O−Al units of the tetrahedral sheet due to the migration of protons at high temperature in a way that can be compared with the effect proposed for vermiculite when it is submitted to acid washing and then to calcination (del Rey-Perez-Caballero and Poncelet, 2000).

Structural elements extracted during hydrolysis are expected to be eliminated through acid washing. Some may remain in the clay, however, as extra-framework species (del Rey-Perez-Caballero and Poncelet, 2000) at exchange positions (del Rey-Perez-Caballero and Poncelet, 2000) or in vacant spaces in the structure (Komadel *et al.* 2005). The increase observed in the ^{VI}Al species by NMR after acid washing is evidence of such behavior. Although the species may remain on the surface of the solid after acid washing (del Rey-Perez-Caballero and Poncelet, 2000; Triantafillidis, 2000), the Al extracted from tetrahedral positions during the HTT process may also migrate, due to its small ionic radius, toward the nearest surface. In the present case, they migrate to the vacancies in the octahedral sheet (Komadel *et al.*, 2005). This characteristic could be related to the Tamman temperature of Al (350ºC) (Wachs, 2005), as, under the optimal HTT conditions, the temperature selected (400ºC) would allow Al to overcome this condition of mobility in the solid state and to be disseminated through the vacant spaces available. The result above could also explain the stability found in the ^{IV}Al:^{VI}Al ratio in solids submitted to the HTT process at lower temperatures (Table 4).

The distribution of structural ions at the end of the treatment for solid H400V75 (Figure 11), which was calculated from the XRF composition described by Newman and Brown (1987), shows an ^{IV}Al:^{VI}Al ratio of 2.9, which is very close to that predicted by ^{27}Al NMR, indicating that the Al must be occupying structural positions and not extra-framework positions. If this distribution were different, the charge balance between the structural ions and the interlayer cations would be inadequate (Komadel *et al.*, 2005).

The structural effect of the extraction of laminar ions in vermiculite after the HTT process was also revealed in the XPS analysis of the H400V75 solid with respect to the starting mineral (Table 5): in the tetrahedral sheet due to the shifts in the Si binding energies (0.53 eV) and in the octahedral sheet because of the Mg (0.63 eV), revealing a different chemical environment for these cations in the octahedral sheet.

These results lead to the proposal that the charge-reduction mechanism in vermiculite in the conditions selected is caused by the extraction of up to 25.4% of ^{IV}Al, accompanied by an extraction of up to 11% of the Mg and 36% of the charge compensating cations (Ca^{2+}, Na^+, and K^+) in natural vermiculite. The reduction of the negative global charge in vermiculite by 35% is caused by the HTT process and acid washing. In addition, some of the ^{VI}Al species at the end of the treatment probably remain in structural positions in the octahedral sheet, with the distribution shown in Figure 11.

CONCLUSIONS

The results allow a first approximation of a model for charge-reduction by hydrothermal treatment in vermiculite.

Under the HTT process at optimal conditions (400ºC and relative humidity of 75% in N_2) a reduction of ~35% in negative charge in the vermiculite was achieved by the extraction of both ^{IV}Al (25.4%) and Mg (11%) and of the charge compensators in vermiculite (36%).

The process probably started with the breakup of the O−Mg−O bonds in the octahedral sheet and in the

V

$$[(Si_{3.04}Al_{0.92}Ti_{0.04})(Al_{0.11}Fe^{3+}_{0.35}Fe^{2+}_{0.07}Mg_{2.41}Mn_{0.003})O_{10}(OH)_2]Ca_{0.21}K_{0.05}Na_{0.10}$$

$$0.57\ e^-/O_{10}(OH)_2$$

H400V75

$$[(Si_{3.31}Al_{0.65}Ti_{0.04})(Al_{0.22}Fe^{3+}_{0.37}Fe^{2+}_{0.07}Mg_{2.15}Mn_{0.003})O_{10}(OH)_2]Ca_{0.16}K_{0.03}Na_{0.03}$$
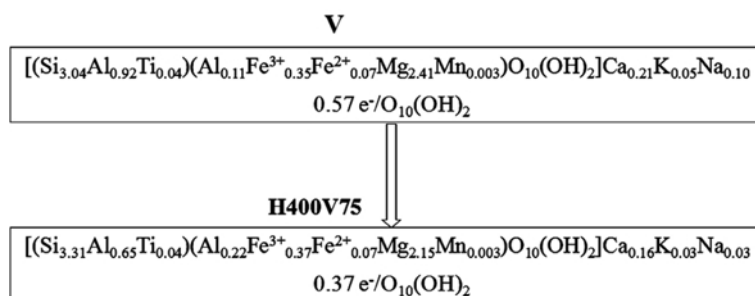
$$0.37\ e^-/O_{10}(OH)_2$$

Figure 11. Structural formula and total charge, obtained by XRF analysis, of the initial vermiculite (V), and for the sample subjected to the HTT process under the conditions H400V75.

Si−O−Al units of the tetrahedral sheet. During acid washing, some of the structural elements extracted were eliminated. However, at the end of the treatment some of the ^{VI}Al species probably remained in the solid in structural positions of the clay in the octahedral sheet.

ACKNOWLEDGMENTS

REFERENCES

Barr, T., Seal, S., Wozniak, K., and Klimowski, J. (1997) ESCA studies of the coordination state of aluminum in oxide environments. *Journal of Chemical Society Faraday Transactions*, **93**, 181−186.

Campos, A. (2007) Estudio del efecto de disminución de carga interlaminar de una vermiculita y su aplicación como catalizadores ácidos tipo arcilla pilarizada. PhD thesis, Universidad Nacional de Colombia, Colombia, 205 pp.

Campos, A., Moreno, S., and Molina, R. (2005) Acidez e hidroisomerización de heptano en una vermiculita colombiana modificada con aluminio. *Revista Colombiana de Química*, **34**, 79−92.

Campos, A., Moreno, S., and Molina R. (2008) Relationship between hydrothermal treatment parameters as a strategy to reduce layer charge in vermiculite, and its catalytic behavior. *Catalysis Today*. **133−135**, 351−356.

Chapman, H. (1965) Cation exchange capacity. Pp. 891−901 in: *Methods of Soil Analysis* (C. Black, D. Evans, J. White, L. Ensminger, and E. Clark, editors). Agronomy **9**, American Society of Agronomy.

Chmielarz, L., Kus'trowski, P., Michalik, M., Dudek, B., Piwowarska, Z., and Dziembaj R. (2008) Vermiculites intercalated with Al_2O_3 pillars and modified with transition metals as catalysts of DeNOx process. *Catalysis Today*, **137**, 242−246.

Chorom, M. and Rengasamy, P. (1996) Effects of heating on swelling and dispersion of different cationic forms of a smectite. *Clays and Clay Minerals*, **44**, 783−790.

Cristiano, D., Campos, A., and Molina R. (2005) Charge reduction in a vermiculite by acid and hydrothermal methods: A comparative study. *Journal of Physical Chemistry B*, **109**, 19026−19033.

d'Espinose de la Calleire, B. and Fripiat, J. (1991) Dealumination and aluminium intercalation of vermiculite. *Clays and Clay Minerals*, **39**, 270−280.

del Rey-Perez-Caballero, F. and Poncelet, G. (2000) Microporous 18 Å Al-pillared vermiculites: preparation and characterization. *Microporous and Mesoporous Materials*, **37**, 313−327.

Giudici, R., Kouwenhoven, H., and Prins, R. (2000) Comparison of nitric and oxalic acid in the dealumination of mordenite. *Applied Catalysis A*, **203**, 101−110.

González, A., Espinòs, J., Munuera, G., Sanz, J., and Serratosa J. (1988) Bonding-state characterization of constituent elements in phyllosilicate minerals by XPS and NMR. *Journal of Physical Chemistry*, **92**, 3471−3476.

Hernández, W., Centeno, M., Odriozola, J., Moreno, S., and Molina R. (2008a) Acidity characterization of a titanium and sulfate modified vermiculite. *Materials Research Bulletin* **43**, 1630−1640.

Hernández, W., Moreno, S., and Molina R. (2008b) Modificación y caracterización de una vermiculita colombiana con especies de titanio, zirconio y sulfato. *Revista Colombiana de Química*, **36**, 73−91.

Jiménez de Haro, M., Pérez-Rodríguez, J., Poyato, J., Pérez-Maqueda, L., Ramírez, V., Justo, A., Lerf, A., and Wagner, F. (2005) Effect of ultrasound on preparation of porous materials from vermiculite. *Applied Clay Science*, **30**, 11−20.

Kitajima, K., Taruta, S., and Takusagawa, N. (1991) Effects of layer charge on the IR spectra of synthetic fluorine micas. *Clay Minerals*, **26**, 435−440.

Klinowski, J. (1999) Solid-state NMR studies of molecular sieve catalysts. *Chemical Review*, **91,** 1459−1479.

Komadel, P., Madejová, J., and Bujdák J. (2005) Preparation and properties of reduced-charge smectite − A review. *Clays and Clay Minerals*, **53**, 313−334.

Madejová, J., Bujdák, J., Janek, M., and Komadel, P. (1998) Comparative FT-IR study of structural modifications during acid treatment of dioctahedral smectites and hectorite. *Spectrochimica Acta A*, **54**, 1397−1406.

Madejová, J., Bujdák, J., Petit, S., and Komadel, P. (2000) Effects of chemical composition and temperature of heating on the infrared spectra of Li-saturated dioctahedral smectites. (I) Mid-infrared region. *Clay Minerals*, **35**, 739−751.

Maqueda, C., Santas Romero, A., Morillo, E., Pérez-Rodríguez, J.L., Lerf, A., and Ernst Wagner, F. (2008) The behaviour of Fe in ground and acid-treated vermiculite from Santa Olalla (Spain). *Clays and Clay Minerals*, **56**, 380−388.

Marques, J., Gener, I., Ayrault, P., Bordado, J., Lopes, J., Ramôa, R., and Guisnet, M. (2005) Dealumination of HBEA zeolite by steaming and acid leaching: distribution of the various aluminic species and identification of the hydroxyl groups. *Comptes Rendus Chimie*, **8**, 399−410.

Michot, L., Tracas, D., Lartiges, B., Lhote, F., and Pons, C. (1994) Partial pillaring of vermiculite by aluminium polycations. *Clay Minerals*, **29**, 133−136.

Moreno, S., Sun Kou, R., and Poncelet, G. (1996) Hydroconversion of Heptane over Pt/Al-pillared montmorillonites and saponites. A comparative study. *Journal of Catalysis*, **162**, 198−208.

Moreno, S., Sun Kou, R., and Poncelet G. (1997) Influence of preparation variables on the structural, textural, and catalytic properties of Al-pillared smectites. *Journal of Physical Chemistry B*, **101**, 1569−1578.

Newman, A. and Brown, G. (1987) The chemical constitution of clays. Pp. 1−128 in: *X−ray diffraction and the Identification and Analysis of Clay Minerals* (D.M. Moore and R.J. Reynolds, editors). Oxford University Press, New York.

Sing, K., Everett, R., Haul, R., Moscou, L., Pierotti, R., Rouquerol, J., and Siemienwska, T. (1985) Reporting physisorption data for gas/solid systems with special reference to the determination of surface area and porosity. *Pure and Applied Chemistry*, **57**, 603−619.

Triantafillidis, C., Vlessidis, A., and Evmiridis, N. (2000) Dealuminated H-Y zeolites: Influence of the degree and the type of dealumination method on the structural and acidic characteristic of H-Y zeolites. *Industrial and Engineering Chemistry Research*, **39**, 307−319.

Tunega, D. and Lischka, H. (2003) Effect of the Si/Al ordering on structural parameters and the energetic stabilization of vermiculites − a theoretical study. *Physics and Chemistry of Minerals*, **30**, 517−522.

Wachs, I. (2005) Recent conceptual advances in the catalysis science of mixed metal oxide catalytic materials. *Catalysis*

Today, **100**, 79−94.

Wagner, C. (1990) *Practical Surface Analysis*. 2nd edition. J. Wiley and Sons, New York.

Wiewióra, A., Perez-Rodriguez, L., Perez-Maqueda, L., and Drapala, J. (2003) Particle size distribution in sonicated high- and low-charge vermiculites. *Applied Clay Science*, **24**, 51−58.